Conservation of ethnographic artefacts: selective laser ablation of deposits from doum palm fibers

Daniele Ciofini[1], Ahmed Bedeir[2], Iacopo Osticioli[1], Abdelrazek Elnaggar[3], Salvatore Siano[1]*

[1] *Istituto di Fisica Applicata ''N. Carrara'', Consiglio Nazionale delle Ricerche, Via Madonna del Piano 10, 50019 Sesto Fiorentino, Florence, Italy*

[2] *Conservation Department, Faculty of Archaeology, South Valley University, Egypt*

[3] *Conservation Department, Faculty of Archaeology, Fayoum University, Egypt*

* Corresponding author: S.Siano@ifac.cnr.it

Keywords: laser cleaning; fluorescence spectroscopy; Raman spectroscopy; photobleaching; vegetable fibers; lignin.

Abstract

This work approaches the challenging cleaning problem of fragile ancient ethnographic artefact crafted using lignocellulosic fibers, which undergo different and concomitant degrading reactions (oxidation, hydrolysis, depolymerization) over time. Here, the fundamental wavelength and second harmonic of QSwitched Nd:YAG laser were comparatively tested for the removal of deposits (soot, dirt, aluminum silicates, carbonaceous material) from an woven-fibers `angarêb, which is exhibited at the Africa Hall of the National Geographic Society Museum (Cairo, Egypt). Besides fiber identification, laser inducedeffects were assessed on `angarêb fibers and fresh, naturally and artificially aged doum palm (*Hyphanae Thebaica*) reference samples by means of stratigraphic examination, UV-induced Vis fluorescence emission, Raman spectroscopy, ESEM-EDX analysis and optical microscopy observations. Irradiation at 532 nm affected color appearance and structural integrity of the fibers. Bond-breaking/depolymerization and bleaching occur at this wavelength, due to the significant absorption of lignin/phenolic-carbohydrate and lignin-quinonoid complexes. In contrast, laser irradiation at 1064 nm did not induce any detectable discoloration or structural alteration, either in the short or long term diagnostic assessments. Raman spectroscopy allowed revealing a slight dehydration of cellulose moieties soon after the laser treatment, which was recovered in the long term ageing tests, which re-established the moisture equilibrium. Thus, the results achieved using 1064 nm, in term of chemical and structural integrity, highlight the possibility of using this wavelength for recovering the original surface of soiled ethnographic artefacts made of vegetable fibers, which are otherwise untreatable.

1. Research aim

The maintenance of artefacts crafted using vegetable fibers represents a very difficult task because of the serious deterioration phenomena they typically present. Besides the need of controlled exhibition conditions, the main conservation aspect concerns the removal of soot accumulated through the fibers, whose brittleness makes very armful any chemical or mechanical action. Exogenous materials incorporated during the use of the objects, their storage or museum exhibition affect the legibility of the manufacturing details and accelerate the deterioration processes. Here, we aimed at thoroughly investigating the laser ablation approach for safe contactless cleaning of such a class of ethnographic artefacts. The potential of the laser approach was explored for the first time on sample of a typical Sudanese bed (`angarêb) of 19th century from the National Geographic Museum of Cairo made of palm

fibers. Irradiation tests using the fundamental wavelength (1064 nm) and the second harmonic (532 nm) of Nd:YAG laser were carried out on both authentic and prepared samples in order to optimize the treatment and achieve general criteria, which could be exploited for the broad class of palm fiber objects.

2. Introduction

Ethnographic objects of a given cultural group include various types of household items crafted using vegetable fibers, such as basketry, matting, ropes, brooms, brushes, textiles, sleeping mats, and many others. For their production, many grass-like plant species (reeds, palms, cereals, and other) have been used among the various cultures along the centuries. Parts of the plants (leaves or leaflets, branches, culms, stem) were and, in some cases, still are (living traditions) accurately selected and then processed using different techniques, such as drying, retting, beating, cooking, and combing. Depending on the final use of the object, twisting, spinning, plating and weaving methods were then used to process fibers in form of yarns, strands, and then ropes [1][2][3][4][5]. Furthermore, very coarse materials such as striped leaves, stems, or other have often been employed for producing emergency cordage or construction rope without any specific preparation [6].

This type of the handicraft production represents a fundamental part of the material culture of population groups of the past, which enrich the ethnographic and anthropological knowledge on their technologies and customs and must hence be preserved for the future generations. However, considering the relatively high perishable nature of lignocellulosic materials, the conservation of the mentioned objects represents a challenging task even when their macroscopic morphology is apparently preserved. Several aspects must be taken into account whenever restoring rare ethnographic findings because of the various and complex deterioration phenomena which are often encountered. The most common are related with the presence of moisture, air pollutants, acid and oxidative agents, trace of transition metal ions, long light exposure, and microorganisms (fungi and erosion bacteria) [7][8][9][10]. Cellulose and hemicellulose moieties and in lesser extent lignin undergo different and concomitant degrading reaction (oxidation, hydrolysis, depolymerization) leading to brittleness of the fibers and overall fragility of the object, which get hence easily alterable during cleaning treatments based on wet methods and alkali [11]. It was found that the drying process from an aqueous medium in air alters the cellulose structure irreversibly [12]. Similarly, the cleaning of aged woven plant fibers by means of mechanical actions using scalpel, air flow, brush, needle, and micro-aspirator can often be time-consuming and invasive, although in the long term dry cleaning is safer than wet technique for easily hydrolisable carbohydrates.

This picture shows the present conservation problem is substantially open. An effective dry cleaning treatment should not involve relevant mechanical actions and be able to remove exogenous materials contributing to the deterioration dynamics (ex. loss of hydrolysable carbohydrates components and other oxidation processes catalyzed by iron ions). At the same time it should not increase the acidity of the fibers, which should be lowered using suitable deacidificants when needed.

Within this framework, the exploration of laser ablation potential appears very motivated. As shown in many studies (see for example [13] and references therein), this technique, if accurately optimised, can be very selective and self-limiting even when used for uncovering incoherent surface layers. However, works dealing with the study of laser interaction with wooden artefacts are relatively a few [14][15][16][17], whilst those regarding archeological plant fibers are decidedly very rare [10, 18].

In the present work, the potential of nanosecond laser ablation for de-soiling ancient plant fiber artefacts was explored for the first time. The fundamental wavelength and second harmonic of Q-Switched

Nd:YAG laser, were comparatively tested in order to remove brown-dark crusts (soot, dirt, aluminum silicates, carbonaceous material) from twisted fiber samples taken from an ancient `angarêb, a wooden framed bedstead, from the Africa Hall of the National Geographic Society Museum (Cairo, Egypt). Significant efforts were dedicated and to identify the fiber type constituting the present bedstead and to characterize soiling material in order to optimize the irradiation parameters and cleaning procedure for its restoration. Laser induced effects at both wavelengths were hence thoroughly investigated through irradiation test of authentic `angarêb rope samples and doum palm (*Hyphanae Thebaica*) fibers prepared samples. UV-induced Vis fluorescence, Raman spectroscopy, thin sections, ESEM-EDX analysis, and optical microscopy were the main techniques used in order to characterise material composition and assess the laser treatments. Finally, the long term stability of laser treated fibers was also investigated.

3. Materials and Methods

3.1 The artefact

The wooden framed bedstead `angarêb (Fig. 1) is a traditional piece of furniture with long history in Sudan dated back to the ancient Kerma culture 1750-1550 BC [19][20]. Nature plant fibers, especially palm leaves which were easily available and relatively inexpensive, were geometrically woven in order to craft the bedstead.

According to the available historical information, the low sleeping rest-place with no headboard [21] under study (`angarêb, Cat. No 351, L ~180cm x W ~80cm x H ~35cm) belonged to the King Munza of Mangbetu who visited Cairo in 1870. The object is composed of connected wooden frame mounted on four legs with a strong network of two-stranded ropes stretched across the bed frame in order to craft a sort of fresh mattress [19]. In particular, any single string or rope is constituted of two bundles of twisted fibers (2 plies) woven in S-twist shape. Four rope fragments of the mentioned artefact of about 4-6 cm each were set available for the present study by the mentioned responsible institution.

3.2 Preparation of Doum Palm samples for systematic irradiation tests

Fresh and natural-dried leaves harvested from mature doum palm *(Hyphaene thebaica, Arecaceae family)* [1], were selected in order to prepare a set of reference samples for systematic irradiation tests. Physical and chemical modification were investigated both on adaxial surface of the leaves, which did not undergo any processing, and on leaves with epidermis stripped off. In detail, the latter were individually handwashed several times in distilled water in order to remove most of the mineral particles on the surface and to soften the mineralised tissue. After this pre-treatment, the leaves were scraped off and their fibers manually extracted using a wooden tool. These fibers were then left to dry at room temperature before being cut to the desired length, bundled, placed on a glass slide, and glued at their edges with double sided adhesive tape. Afterwards, a set of the leaf and fiber samples was artificially aged according to UNI ISO 5630-3 (6 days, 80 °C, RH 65%, absence of light) [8].

This aging treatment was selected in order to induce bond breaking via hydrolysis mainly to cellulose moieties, although also those of lignin may be affected as well [7],[22],[23],[24]. The different types of samples prepared are listed in Table 1.

Artificial ageing was also used in order to evaluate long-term side effects after laser irradiation. In this case slightly softer conditions were used: 6 days, 60 °C, RH=50%.

3.3 Analytical samples

Transverse and longitudinal thin sections (TS and LS, respectively) were prepared, according to the well-established procedure for treating the present vegetable samples [25]. 12 single fibers taken by the an `angarêb rope were accurately selected, cut along the transverse direction into small portions (3 mm length) and fixed for 12 h at 4°C in a solution of 3% (w/v) glutaraldehyde in phosphate buffer at pH 7.1. They were then dehydrated in an ethanol series, and embedded in Epon/Araldite epoxy resin, which was polymerized for 24 h at 60 °C. Afterwards, samples T and L sections were cut from embedded material, using an ultra sliding microtome.

Surface and cross-section microscopic appearance was also examined with environmental scanning electron microscopy (ESEM Model: Quanta-200 FEI) by using single fibers (long 3 mm), which were frozen using a Peltier prior to be cut and analyzed. Gold coated samples of reference natural plant fibers such, as Asbestos, Coir, Cotton, Linen, Papyrus, Hemp, Jute, Silk, Sisal, straw and wool were also prepared for microscopic investigation (SEM Philips XL 30, accelerating voltage 30 kv, resolution 3.5 nm) in order to aid the identification of `angarêb fibers.

3.4 Chemical and physical characterizations

UV-induced Vis fluorescence (UV-Vis-Fluo), Raman and FTIR spectroscopies, and ESEM-EDX microanalysis were used to characterize molecular features and composition of plant fibers and soiling before and after laser irradiation. Furthermore, a compact digital microscope (DM) with 500 x video magnification was constantly used during the tests for directly monitoring the sample surface under laser irradiation.

A suitable setup including a standard epi-fluorescence microscope (Nikon Eclipse E400) equipped with a mercury arc lamp,V-2A filter cube (EX: 380–420 nm; DM: 430 nm; BA: 450 nm), and a co-axial fiber optic spectrometer (200-1100 nm, grating 300 lines/mm) was assembled to measure UV-Vis-Fluo spectra. The blue excitation range includes the line at 404.7 nm of mercury, which mostly excites the fluorescence of epidermis but also that of mesophyll cells. A 20□ objective lens (field of view 1 mm), ND density filters, integration time of 500 ms and 3 averaging corresponded to the optimal condition for avoiding self-quenching. In order to determine the area, width, and λ_{max} of fluorescence band, a Gaussian fit was applied to each spectrum. To improve the signal to noise ratio 10 points of SG smoothing filter was also applied.

A homemade Raman system (exc. 1064 nm) equipped with a deep-cooled (-60°C) spectrometer (InGaAs array detector) covering spectral range between 165-1825 cm^{-1} was used. This instrument includes an automated control of the laser energy release to the target in order to prevent undesired overheating effects within the irradiated volume [26],[27]. Three different spots in each irradiated area were measured.

3.5 Laser irradiation tests

The fundamental wavelength (1064 nm) and the second harmonic (532 nm) of a Q-Switched Nd:YAG laser (pulse duration of 11 ns) were used to irradiate the samples through optical fiber and imaging lens [9]. Laser irradiation tests aimed at determining the ablation threshold (F_{th}) of the encrustation distributed on authentic rope samples were preliminary performed using both the mentioned laser wavelengths. F_{th} was defined as the lowest fluence at which ablation texturing of the stratification layer was observable

under the optical microscope and ESEM. Afterwards, areas of 5□5 mm^2 were systematically irradiated at F_{th}, $2F_{th}$, and $4F_{th}$, respectively, using laser pulse trains and by step-by-step translation (with a minimal overlapping) of the sample under the laser beam. Two alternative time exposure and pulse repetition rates were used for achieving each cleaning spot (□ 1.4 mm): 10 s, 2 Hz and 2 s, 10 Hz, respectively. The same methodology was applied to the prepared samples listed in Table 1, in order to study possible chemical or physical changes induced by laser irradiation. Leaf samples were irradiated only on adaxial surface. Energy meter (Lab Max, Coherent) and neutral density filters were used to finely select the desired fluence.

4. Results

4.1 Identification of the vegetable fibers

The `angarêb fragments analyzed were seriously deteriorated, brittle and soiled. No decorative marks or pigment applications were detected by visual and microscopic investigations. In order to identify vegetable fibers used, a preliminary electron microscopy comparison with coir, hemp, jute, sisal, straw, and asbestos fibers was carried out. However, no morphological matches were found and the presence of deposits did not allow achieving more detailed information on the authentic ancient fiber.

Deeper anatomical examinations were possible after the early cleaning tests according to the methodology described below. Figure 2 reports ESEM images of single TS and adaxial `angarêb fiber. showing some peculiar details which allowed identifying the plant. The diameter of the fiber was approximately 300 μm and embedded silica bodies, ranging between 10 and 25 μm, were located beneath the outer epidermis. Closer ESEM inspections revealed spherical phytoliths with pointed and rounded spinules, flat apex and regular distribution in length. These features are ascribable to the Doum palm (*Hyphaene thebaica*), a desert palm native to Egypt, sub-Saharan Africa and West India [28]. This along with date palm L., Cyperus papyrus L., and D. bipinnata were and are still used today in manufacture of ropes, baskets, and bags [28], [29].

TS microphotographs of lamina taken under transmitted light and fluorescence microscope are reported in Fig. 3, which show the anatomy of the fiber. The mesophyll, a part of the inner tissue (parenchyma) of a leave containing many chloroplasts, was not well differentiated into palisade and spongy layers, according to the literature [5]. The lamina, formed by two superimposed layers of epidermis cells forming a undulate profile, enclosed the multicellular fibrovascular bundles, the thick-walled lignified sclerenchyma cells [30][31]. Vascular bundles, in doum palm are organized perpendicularly to the longitudinal axis of the leaf [32], [33]. Intermediate fiber bundles, which cover around ½ of the distance across the mesophyll, are adaxial. Under violet excitation, the epidermal layers together with vascular bundles are characterized by intense light blue-green fluorescence due to phenolics (i.e. mostly hydroxicinnamic acids) bound to cell walls of epidermal cells and fiber vascular bundles, while the mesophyll is not longer fluorescent [34].

4.2 Chemical characterization of the ancient fibers

FT-IR analysis of raw fibers showed a broad and intense band at 3000 - 3500 cm^{-1} indicating the material was strongly degraded by acidic compounds containing OH groups. Stretching vibrations of −CH and $-CH_2$ groups of cellulose were detected at 2920 and 2852 cm^{1} , whereas typical minor bands associated with the symmetrical deformation of −CH in lignin and α-cellulose were no longer detectable [31]. Lignin

likely provided the main contribution to the bands at1650 and 1518 cm^{-1} (conjugated C=O and C=C of the aromatic ring), although the former also included the contribution of the HOH bending vibration of adsorbed water. The high amount of lignified cells in detriment of cellulose and hemicellulose moieties due to the advanced degradation were testified by the reduced intensity of the bands at 1383 and 1318 cm^{1}, which are assigned to CH bending and wagging of cellulose and CO stretching of guaiacyl, and syringyl lignin [35] , respectively.

A significant presence of lignin-derived aromatic compounds was detected in Raman spectra through υ(C=C) vibration. In particular, the most intense peak observed at 1609 cm^{-1} and related shoulder at 1635 cm^{-1} were ascribed to phenyl ring stretching and alkene structures present in lignin [36], [37], [38]. The bands observed at 1172, 1125, 1098 cm^{-1} were mainly associated to CH and CO stretching vibrations in cellulose moieties [39][40].

Local EDX analysis of the encrustation allowed pointing out the soiling was composed of sodium, aluminum silicates along with Fe, Cl, K, S, Mg, which are the typical elemental markers of the Egyptian soil [10], [41].

Finally, the fluorescence of the inner fibers of the `angarêb rope, where no significant presence of soiling was observed under the DM, was at about 548 nm. In contrast, the fluorescence of external encrusted fibers was blue-shifted at 492 nm, thus suggesting the presence of exogenous organic components.

4.3 Laser irradiation effects on reference samples

Once `angarêb fibers were characterized and identified, chemical and physical modifications induced by 1064 and 532 nm laser irradiations were preliminary assessed on reference leaf samples by means of UV-Vis-Fluo measurements along with DM and ESEM examinations. The irradiation parameters were those used for cleaning soiled areas of `angarêb ropes. Figure 4 shows UV-Vis-Fluo spectra of FL and HAL samples collected from the same test area before and after laser irradiation. As shown, remarkable increases in intensity of fluorescence signal associated with narrowing were noticed in laser irradiated spots using 532 nm, $2F_{th}$ and $4F_{th}$ fluences, and prr 10 Hz. The increase of fluorescence emission observed at the highest fluences was also associated with visible bleaching without any microstructural change of adaxial surface. Very surprisingly, chromatic recover of bleached spots was observed in all the irradiated areas after a few weeks. In contrast, no evidence of such changes was observed at 1064 nm (Fig. 4c-d).

The structured low-energy bands with maximum centered at 680 nm and relative shoulder at about 720 nm of the spectra displayed in Fig. 4, are ascribable to the chlorophyll *a*, which was still present and detectable in some extent in FL samples in spite of the significant epidermal screening [42], [43]. In NAL and NALHA samples the chlorophyll *a* was no longer detectable (Fig. 5). It is worth noting that the laser treatment did not affect the chlorophyll fluorescence, although in laser damaged areas at 532 nm it appeared slightly quenched. Spectra of HAL samples (Fig. 4e-h) exhibited similar intensities but they were rather broadened and red-shifted with respect to those of FL.

NAL and NALHA samples exhibited slightly lower increases of UV-Vis-Fluo (Fig. 5) than those recorded for FL and HAL samples (Fig. 4).

Evident laser induced effects start to take place after laser irradiation at 532 nm, $2F_{th}$, and 10 Hz prr, which got more pronounced at $4F_{th}$. As previously found, no evidence of microstructural changes was observed. A similar trend was observed for NAF and NAFHA samples, although they were relatively more sensitive. Irradiation at 532 nm, $4F_{th}$, and 2-10 Hz produced increasing of the fluorescence,

followed by photobleaching of the fibers. In contrast to 532 nm, none of these surface alterations were instead observed at 1064 nm.

4.4 Laser irradiation tests on `angarêb fibers

4.4.1 Microscopy

Laser tests on `angarêb rope fragments were performed by irradiating 0.5x0.5 cm^2. On the basis of ESEM inspections, the F_{th} needed for the complete removal of soiling was found to be about 200 mJ/cm^2 at 532 and 600 mJ/cm^2 at 1064 nm. These values were slightly dependent on the morphology of the site under irradiation as well as on other physical properties of the encrustation layer. With the aim of properly defining safe operative fluence ranges, systematic removal tests on original fibers were carried out at the following fluences: F_{th}, $2F_{th}$, and $4F_{th}$. DM images of the irradiated areas are displayed in Fig. 6. Although the physical condition of the fibers beneath the crust was formerly unknown, the examination provided evidence that irradiation at 532 nm at F_{th} and 2-3 Hz prr did not affect the integrity of the fibers, whereas at $2F_{th}$ (and $4F_{th}$), and 10 Hz prr mechanical damages and peeling of the residual leaf epidermis and hypodermis were observed. Closer inspections at ESEM revealed that epidermis layers were mechanically and thermally affected by laser radiation and in some cases the veins were uncovered. Conversely, irradiation at 1064 nm produced very respectful uncovering results. Complete and selective removal of the stratification was achieved at F_{th} (0.6 J/cm^2), $2F_{th}$ and $4F_{th}$ (prr: 2-10 Hz) and the natural chromatic and morphological features were safeguarded. Damage threshold at 1064 nm was above the tested fluences.

As regards the surface composition of laser-treated fibers, EDX analysis confirmed the effectiveness of both the laser wavelengths in the removal of the main elements constituting the soiling, including iron, which is known as one the most efficient catalyst for accelerating oxidation and hydrolysis reaction in acidic environment.

4.4.2 UV-induced Vis fluorescence

UV-Vis-Fluo spectra of `angarêb fibers treated at 532 and 1064 nm, respectively, are displayed in Fig. 7. Generally, intensity of fluorescence emission in treated/cleaned fibers with both the laser wavelengths tended to increase up to 20-25 $\mu W/cm^2/nm$ (close to the emission of non-soiled inner fibers of the ropes) due to the gradual removal of soiling, An opposite trend was instead measured in fibers treated at 532 nm with $4F_{th}$ and 10 Hz. The decrease/quenching of the fluorescence at increasing fluences may be associated with the onset of charring, in accordance with what observed in reference NAFHA samples. Most importantly, FWHM of fluorescence bands of areas treated at 532 nm was reduced of about 20 nm. The observed shortening of the fluorescence was due to the modification of alkene/aromatic compounds (carotenoids like β-carotene, lycopene and quinoid structures) in non-aromatic compounds. This change is also associated with a visible bleaching of the fibers. Irradiation at 1064 nm did not induce any modifications to fluorescence spectra, neither in peak positions nor in shape. Furthermore, ageing after 1064 nm laser treatment did not induce relevant changes in fluorescence spectra (Fig. 7e-f), thus strengthening the evidence of effectiveness.

4.4.3 Raman spectroscopy

Raman spectra of non-exposed and laser-exposed `angarêb samples are compared in Fig. 8. Expectedly, upon irradiation at 532 nm remarkable changes were observed. The bands ascribed to υ(C=C) in lignin

and related aromatic units (phenols), as well as those of the υ(C-C and C-O) bonds in cellulose gradually disappeared at increasing fluences due to photobleaching. At $4F_{th}$ with 2 and 10 Hz any (data not shown) spectral features was completely lost. On the other hand, laser-induced cleavage by photolysis or overheating may affect seriously lignin/phenolic–carbohydrate complexes leading to their fragmentation and depolimerization, in accordance with what argued using UV-Vis-Fluo spectra.

Conversely, at 1064 nm intensities of Raman bands increased with fluences thus returning similar spectra as those of the inner non-soiled fibers, which were selected as a reference of the final goal of the laser treatment. Specifically, bands related to cellulose at 1172, 1125, 1098 cm^{-1} [39] increased in intensity while those assigned to lignin went closer to non-soiled reference. In order to better clarify the enhancement in cellulose band intensity and more importantly, to assess long-term stability of `angarêb fibers after treatment at 1064 nm, samples were exposed to a cycle of hydrothermal ageing (6 days, T=60 °C, R.H=50%).

In non-soiled `angarêb fibers further ageing produced negligible modification of bands related to cellulose moieties, which are more easily hydrolysable. In turn, long-term ageing effects on fibers treated at 1064 nm demonstrated the benefits of laser treatment at the highest fluence tested ($4F_{th}$). Basically, areas treated at 1064 nm at F_{th} exhibited lower signals with respect to those irradiated at $2F_{th}$ and $4F_{th}$ (Fig. 8d-e). The latter was very similar to non-soiled fibers, although cellulose peaks showed lower intensities. For a better comparison, the intensity ratio between 1608 (assigned to lignin) and 1098 cm^{-1} (assigned to cellulose) peaks is reported in table 2. The drastic reduction of the Raman bands after accelerated ageing of samples treated at F_{th} is reasonably attributable to the insufficient removal of the crust, which was associated to a consequently higher surface reactivity. Residual pollutants likely underwent reactions with water and substrates, as well as redistribution driven by hydration and exudation of waxy material. As a matter of fact, after hydrothermal ageing, the area previously treated at F_{th} appeared relatively darker under optical microscope with respect to those uncovered using $2F_{th}$ and $4F_{th}$. The latter fluence completely removed exogenous materials thus favoring the stability of the fibers and the detection of their Raman bands.

5. Discussion

5.1 Characterization of `angarêb fibers

Preliminary investigation aimed at analyzing and identifying `angarêb fibers pointed out the presence of silica bodies and lamina anatomical characters ascribable to Doum palm (*Hyphaene thebaica*).

Although silica bodies of more than one type may be present in a single species, in grass taxonomy (including palms), the shape, frequency, and distribution of silica bodies of the mature leaf are combined with other properties of the epidermis for identifying taxonomically subfamily and lower levels [44]. Closer ESEM inspections revealed spherical phytoliths (Fig. 2) with pointed and rounded spinules (called echinate), flat apex and regular distribution in length. Spherical to elliptical and conical to hat-shaped phytoliths are usually found in the *Arecaceae* (palms) and *Bromeliaceae* [45]. However, in *Arecaceae* (palms) the spinules are often very regular in distribution and better defined than in *Bromeliaceae*. Furthermore, palm genera have predominantly pointed and rounded spinules with phytoliths size ranging from about 6 up to 25 µm. Bromeliad has phytoliths much smaller, varying from less than 2 µm to about 10 µm in diameter. At same time, transmitted light and fluorescence microscopies showed not differentiated mesophyll into palisade and spongy tissues, the presence of peltate hairs and intermediate

veins with fibrous sheath extensions attached to both surfaces (adaxial and abaxial) forming a girder type vein [5]. These and other anatomical characters allowed to identify precisely the fibers used to craft the present `angarêb.

Besides fiber identification, many other important features related to structural and chemical integrity of the fibers were pointed out. From a conservation standpoint, the `angarêb fragments analyzed were dehydrated, wrinkled, brittle and soiled. Furthermore, inspections of fibers presenting a longitudinal cut showed epidermal cells very encrusted, which suggest the fibers were probably dried, cut and then beaten, before to be assembled as ropes.

Chemically, FTIR spectroscopy of raw fibers showed several overlapping bands because of the multicomponent nature of lignocellulosic materials. As a consequence, only the contribution of the major components, among which lignin followed by cellulose, could be appreciated. Moreover, FTIR analysis evidenced the material was strongly degraded/depolymerized by acidic compounds containing OH groups. Similarly, Raman showed the strong peaks from lignin-derived aromatic compounds and cellulose, as the other complex chromophore structures (extractives) present in palm leaves tissue were difficult to characterize [38],[39].

Among the encrustation elements pointed out by EDX (Fe, Cl, K, S, Mg), Fe ions were the most harmful, because they easily catalyze via acidic hydrolysis carbohydrates (hemicellulose and cellulose) thus activating the depolymerization of cellulose chains over time [45].

5.2 Laser irradiation

According to microscopic and spectroscopic assessments of the laser-induced effects, distinct phenomena occur upon irradiation at 532 and 1064 nm. Laser tests performed on fresh, naturally and artificially aged reference samples, respectively, either in form of leaves and strips, provided evidence that irradiation at 532 nm produced significant fluorescence increase (Figs. 4-5). Such a chemical alteration was also associated with photo-bleaching. In contrast, no evidence of such changes has ever occurred at 1064 nm.

Besides the increasing in fluorescence intensity, irradiation at 532 nm of `angarêb fibers also led to a narrowing of the main band of about 20 nm and, similarly to leaf samples, treated-fibers appeared brighter than those poorly soiled from the rope core. Such a bleaching phenomenon, which was also observed on old paper [46] is likely produced by laser induced reaction of chromophores, although its complete interpretation still need substantial insights.

The main responsible chromophores at 532 nm can be indirectly argued by comparing fluorescence spectra of NAL and FL samples. In contrast to FL samples (Fig. 4), fluorescence spectra of NAL (Fig. 5) and `angarêb fibers (Fig. 7) did not show any contribution from chlorophyll *a* (fluorescence bands at 680 and 720 nm). By taking into account that in green plants, including monocotyledons, the fluorescence of chlorophyll and flavonoids decreases with ageing of leaf tissues, the remaining fluorescence (450-550 nm) could be ascribed mainly to bound phenolics like hydroxycinnamic acids [43]. Among the latter, bound ferulic acid, which is the precursor of aromatic lignin, is one of the most abundant phenolic phytochemical found in plant cell walls. In particular, ferulic acid linked to cell wall polysaccharides by ester bonds is the major fluorophore identified in most plant species showing intense blue-green fluorescence [47]. Consequently, high concentrations of peripherally located hydroxycinnamic acids impart UV screening properties on living tissues, especially protecting mesophyll [34], [42]. Further contribution to fluorescence emission is also due to carotenoids (i.e.β-carotene) and quinonoid structures which commonly occur in different lignin types [48]. These consideration are crucial as clearly indicate

that the 532 nm wavelength may induce modification (i.e. photo-bleaching) mainly to epidermis bound phenolics, and lignin-quinonoid structures. At high fluences, structural damage to hypodermis may take place. Likewise, Raman spectroscopy highlighted that decomposition of lignin and cellulose takes place at 532 nm with increasing fluences. At $4F_{th}$ with 2 and 10 Hz any spectral feature was completely lost. On the other hand, lignin/phenolic-carbohydrate and lignin-quinonoid complexes are absorbing compounds in the visible range. Therefore, direct photolysis and overheating may lead to fragmentation/depolymerization reaction, in accordance with what pointed out by UV-Vis-Fluo microspectroscopy. It was demonstrated that lignocellulosic materials are sensitive to irradiation in the range from 300 to 400 nm and up to 500 nm for some wood species [49]. Color modification of lignocellulosic materials on UV-Vis light exposure was mainly attributed to lignin, while photobleaching is detected in the visible region due to the photolysis of quinonoid structures [50]. Moreover, depolymerization reactions catalyzed by both acid (typically at 0−200 °C) and base (100−300 °C) break the C−O or C−C linkages between lignin units to produce small segments including monomeric phenols [51].

Conversely, irradiation at 1064 nm of leaf reference and `angarêb samples produced very satisfactory results in terms of color appearance, chemical and morphological structure. Accordingly to UV-Vis-Fluo, no remarkable changes in Raman spectra were observed. Intensities of Raman bands increased steadily with increasing fluences until getting similar to those of non-soiled fibers. Specifically, relative intensities of bands related to cellulose resulted slightly enhanced if compared to those assigned to lignin after laser treatment. Although the cellulose bands in all the regions analyzed were similar in terms of spectral features, intensity variations were observed, which can be attributed to crystalline/amorphous nature of cellulose and its crystallite size in different location, mean fibril angle [52],[53] as well as to inhomogeneous ageing effects. Thus, as a consequence of the variability of lignocellulosic fibers, it is fairly challenging to assess exactly the nature of the intensity increase of C-O and C-C stretching in cellulose chains. In studies carried out on Whatman paper changes in the C-O stretching, ring stretching, and C-O-C asymmetric stretching vibrations in DRIFT spectra were associated with formation of intra- or intermolecular ether bonds [54].

After 6 days of exposure to hydrothermal ageing of the sample cleaned using 1064 nm, no relevant fluorescence changes were observed regardless from fluences and prr. A drastic decrease in the intensity of Raman scattering was observed in areas treated at Fth, which evidenced the need to operate at higher fluences. In poorly cleaned fibers, hydrolysis catalyzed by Fe ions continues, in the long term, to react with the woody substrate, whereas Fe-free fibers after laser treatment at 2Fth or 4 Fth were instead less prone to acidic hydrolysis.

6. Conclusions

The present work represents the first investigation on laser cleaning of doum palm Egyptian `angarêb. Laser induced effects at 532 and 1064 nm were thoroughly studied through cleaning trials of ancient encrusted rope fragments, systematic irradiation tests of prepared samples, and corresponding analytical assessments. The former wavelength efficiently removed exogenous materials using relatively low fluences but it produced narrowing of the main fluorescence band with respect to 1064 nm already at the cleaning threshold (200 J/cm^2) and visible bleaching at higher fluences. This is attributable to undesired chemical effects (bond-breaking/depolymerization) driven by optical absorption of

lignin/phenoliccarbohydrate and lignin-quinonoid complexes, as suggested by the disappearance of the υ(C=C) Raman band at increasing fluences.

Alterations of the fluorescence spectrum were also detected after irradiation of prepared doum palm samples. Significant rises and narrowing of the main fluorescence band were observed when using 532 nm at the maximum fluence of 800 mJ/cm^2 and prr of 10 Hz.

In contrast, irradiation at 1064 nm did not produce any evidence of discoloration or structural alterations, either in the short and long term ageing simulation, even when using relatively high fluences (up to 2.4 J/cm^2). Macroscopic encrustation was selectively removed from `angarêb rope surfaces and residual iron oxides (catalysts of acidic hydrolysis) were minimized. This result discloses a significant application perspective of the laser ablation in preservation of an important part of ethnographic heritage. In contrast to scarcely selective chemical and mechanical methods, optimized laser treatments can represent the most respectful, repeatable, and efficient cleaning approach to a large variety of artefacts crafted using vegetable fibers.

Acknowledgments

The authors gratefully acknowledge the financial support provided by the European project IPERIONCH (H2020, INFRAIA 2014-2015. nº 654028), and Science and Technology Development Fund (Grant No. STDF –STF 6707), the Egyptian Ministry for Scientific Research. Loosen and soiled fragments of the `angarêb ropes were kindly supplied for this study by National Geographic Society Museum (Cairo, Egypt). Many thanks to Maria Cristina Salvatici of the center of electron microscopy "L. Bonzi" (Ce.ME, CNR Florence) for the support in preparing thin sections.

REFERENCES

[1] K. Borojevic, R. Mountain, Microscopic identification and sourcing of ancient egyptian plant fibres using longitudinal thin sectioning, Archaeometry 55 (2013) 81–112. doi:10.1111/j.14754754.2012.00673.x.

[2] N.M. Waly, The selection of plant fibers and wood in the manufacture of organic household items from the El-Gabalein area Egypt, Exploit. Plant Resour. Anc. Africa (1999) 261–272.

[3] C.J.M. Amwatta, Diversity of Use of Doum (Hyphaene compressa), PALMS 48 (2004) 184–190.

[4] T. Romain, Anatomy of the endemic palms of the Near and Middle East: archaeobotanical perspectives, Rev. D'Ethnoécologie 4 (2013) 1–17.

[5] N.M.N. El Hadidi, R. Hamdy, Basketry accessories: Footwear, bags and fans in ancient Egypt, J. Archaeol. Sci. 38 (2011) 1050–1061. doi:10.1016/j.jas.2010.11.026.

[6] C. Isaza, R. Bernal, P. Howard, Use, Production and Conservation of Palm Fiber in South America: A Review, J. Hum. Ecol. 42 (2013) 69–93.

[7] L.M. Proniewicz, C. Paluszkiewicz, A. Wesełucha-Birczyńska, A. Barański, D. Dutka, FT-IR and FT-Raman study of hydrothermally degraded groundwood containing paper, J. Mol. Struct. 614 (2002) 345–353. doi:10.1016/S0022-2860(02)00275-2.

[8] C. Rosati, D. Ciofini, I. Osticioli, R. Giorgi, S. Tegli, S. Siano, Laser removal of mold growth from paper, Appl. Phys. A Mater. Sci. Process. 117 (2014) 253–259. doi:10.1007/s00339-0148507-z.

[9] D. Ciofini, I. Osticioli, S. Micheli, L. Montalbano, S. Siano, Laser removal of mold and foxing stains from paper artifacts: preliminary investigation, in: Fundam. Laser-Assisted Micro-Nanotechnologies, Ed. by V. P. Veiko, T. A. Vartanyan, Proc. SPIE, Vol. 9065, 2013: p. 906512. doi:10.1117/12.2052820.

[10] A. Elnaggar, P. Fitzsimons, A. Nevin, K. Watkins, M. Strlič, Viability of laser cleaning of papyrus: Conservation and scientific assessment, Stud. Conserv. 60 (2015) S73–S81.

[11] R.G. Elenga, P. Djemia, D. Tingaud, T. Chauveau, J.G. Maniongui, G. Dirras, Effects of alkali treatment on the microstructure, composition, and properties of the Raffia textilis fiber, BioResources. 8 (2013) 2934–2949. doi:10.15376/biores.8.2.2934-2949.

[12] R.S. Atalla, M.F. Crowley, M.E. Himmel, R.H. Atalla, Irreversible transformations of native celluloses, upon exposure to elevated temperatures, Carbohydr. Polym. 100 (2014) 2–8. doi:10.1016/j.carbpol.2013.06.007.

[13] S. Siano, J. Agresti, I. Cacciari, D. Ciofini, M. Mascalchi, I. Osticioli, a. a. Mencaglia, Laser cleaning in conservation of stone, metal, and painted artifacts: State of the art and new insights on the use of the Nd:YAG lasers, Appl. Phys. A Mater. Sci. Process. 106 (2012) 419–446. doi:10.1007/s00339-011-6690-8.

[14] M. Panzner, G. Wiedemann, K. Henneberg, R. Fischer, T. Wittke, R. Dietsch, Experimental investigation of the laser ablation process on wood surfaces, Appl. Surf. Sci. 127-129 (1998) 787–792. doi:Doi: 10.1016/s0169-4332(97)00743-5.

[15] G. Wiedemann, M. Schulz, J. Hauptmann, H.-G. Kuscg, S. Muller, M. Panzner, H. Wust, Laser cleaning applied in the restoration of a medieval wooden panel chamber at Pirna, J. Cult. Herit. 3887 (2000) 240–249. doi:10.1016/S1296-2074(00)00133-3.

[16] M. Cooper, M. Solajic, G. Usher, J. Ostapkowicz, The application of laser technology to the conservation of a Haida totem pole, J. Cult. Herit. 4 (2003) 165–173. doi:10.1016/S12962074(02)01142-1.

[17] a. Koss, M. Lubryczynska, J. Czernichowska, I. Uchman-Laskowska, K. Chmielewski, M. Mazur, a. Markowska, J. Marczak, M. Strzelec, Conservation of wooden art works and laser cleaning, 7391 (2009) 73910S. doi:10.1117/12.827516.

[18] R. Belli, A. Miotello, P. Mosaner, L. Toniutti, M. Bazzanella, Preliminary Laser Cleaning Studies of a Consolidated Prehistoric Basketry Coming from the Pile Building of Fiavè-Carera in the North-East of Italy, Laser Chem. 2006 (2006) 1–5. doi:10.1155/2006/64690.

[19] B. Jerbi, The ` angarêb in Northern Sudan, Med. Antropol. 18 (2006) 59–72.

[20] A.K. Aremu, O.K. Fadele, Study of some properties of doum palm fruit (Hyphaene thebaica Mart.) in relation to moisture content, African J. Agric. Res. 6 (2011) 3597–3602. doi:10.5897/AJAR11.247.

[21] E.S. Thomas, Catalogue of the Ethnographical Museum of the Royal Geographical Society of Egypt, Impr. de l'Institut français d'archéologie orientale, Le Caire, 1924.

[22] M. Strlič, J. Kolar, Ageing and stabilisation of paper, National and University Library Ljubljana, 2005.

[23] M. Nuopponen, T. Vuorinen, S. Jämsä, P. Viitaniemi, Thermal modifications in softwood studied by FT-IR and UV resonance raman spectroscopies, J. Wood Chem. Technol. 24 (2004) 13–26. doi:10.1081/WCT-120035941.

[24] M.C. Area, H. Cheradame, Paper aging and degradation: Recent findings and research methods, BioResources 6 (2011) 5307–5337. doi:10.15376/biores.6.4.5307-5337.

[25] H.P.S.A. Khalil, M.S. Alwani, A.K.M. Omar, Chemical composition, anatomy, lignin distribution, and cell wall structure of Malaysian plant waste fibers, BioResources 1 (2006) 220–232. doi:10.15376/biores.1.2.220-232.

[26] I. Osticioli, D. Ciofini, A.A. Mencaglia, S. Siano, Automated characterization of varnishes photodegradation using portable T-controlled Raman spectroscopy., Spectrochim. Acta. A. Mol. Biomol. Spectrosc. (2016). doi:10.1016/j.saa.2016.03.016.

[27] I. Osticioli, A.A. Mencaglia, S. Siano, Temperature-controlled portable Raman spectroscopy of photothermally sensitive pigments, Sensors Actuators B. Chem. 238 (2017) 772–778. doi:10.1016/j.snb.2016.07.104.

[28] A.M. Rosen, Preliminary identification of silica skeletons from Near Eastern archaeological sites: an anatomical approach, in: Phytolith Syst., Springer, 1992: pp. 129–147.

[29] D.R. Piperno, Phytoliths: a comprehensive guide for archaeologists and paleoecologists, Rowman Altamira, 2006.

[30] S. Sghaier, F. Zbidi, M. Zidi, Characterization of Doum Palm Fibers After Chemical Treatment, Text. Res. J. 79 (2009) 1108–1114. doi:10.1177/0040517508101623.

[31] S. Zannen, L. Ghali, M.T. Halimi, M. Ben Hssen, Effect of Chemical Extraction on Physicochemical and Mechanical Properties of Doum Palm Fibres, (2014) 203–216.

[32] R. Thomas, D. De Franceschi, Palm stem anatomy and computer-aided identification: The coryphoideae (Arecaceae), Am. J. Bot. 100 (2013) 289–313. doi:10.3732/ajb.1200242.

[33] V. Bucur, Springer Series in Wood Science Springer Series in Wood Science, 2003. doi:10.1007/978-3-662-08986-6.

[34] A. Solovchenko, Photoprotection in plants: optical screening-based mechanisms, Springer Science & Business Media, 2010.

[35] J.I. Hedges, R.M. Rowell, R.J. Barbour, The chemistry of archaeological wood., in: Archaeol. Wood Prop. Chem. Preserv., American Chemical Society, 1990: pp. 111–140.

[36] M. Nuopponen, S. Willför, a. S. Jääskeläinen, a. Sundberg, T. Vuorinen, A UV resonance Raman (UVRR) spectroscopic study on the extractable compounds of Scots pine (Pinus sylvestris) wood: Part I: Lipophilic compounds, Spectrochim. Acta - Part A Mol. Biomol. Spectrosc. 60 (2004) 2953–2961. doi:10.1016/j.saa.2004.02.008.

[37] M. Takayama, T. Johjima, T. Yamanaka, H. Wariishi, H. Tanaka, Fourier transform Raman assignment of guaiacyl and syringyl marker bands for lignin determination, Spectrochim. Acta Part A Mol. Biomol. Spectrosc. 53 (1997) 1621–1628. doi:10.1016/S1386-1425(97)00100-5.

[38] U.P. Agarwal, An overview of Raman spectroscopy as applied to lignocellulosic materials, Adv. Lignocellul. Charact. (1999) 201–225. http://128.104.77.228/documnts/pdf1999/agarw99a.pdf.

[39] U.P. Agarwal, S. a. Ralph, FT-Raman spectroscopy of wood: Identifying contributions of lignin and carbohydrate polymers in the spectrum of black spruce (Picea mariana), Appl. Spectrosc. 51 (1997) 1648–1655. doi:10.1366/0003702971939316.

[40] A.S. Jaaskelainen, A.M. Saariaho, J. Vyorykka, T. Vuorinen, P. Matousek, A.W. Parker, Application of UV-Vis and resonance Raman spectroscopy to study bleaching and photoyellowing of thermomechanical pulps, Holzforschung 60 (2006) 231–238. doi:10.1515/HF.2006.038.

[41] A.A. Elnaggar, P. Pouli, A. Nevin, M.A. Fouad, G.A. Mahgoub, Laser cleaning of burial encrustation and aged protective coating on Egyptian leather: Optimization of working conditions, Lasers Conserv. Artworks VIII (2010) 39.

[42] E.E. Pfündel, G. Agati, Z.G. Cerovic, Optical properties of plant surfaces, in: C. Müller, M. Riederer (Eds.), Biol. Plant Cuticle, Blackwell Publishing Ltd, 2006.

[43] S. Meyer, a. Cartelat, I. Moya, Z.G. Cerovic, UV-induced blue-green and far-red fluorescence along wheat leaves: A potential signature of leaf ageing, J. Exp. Bot. 54 (2003) 757–769.

doi:10.1093/jxb/erg063.

[44] P.C. Twiss, E. Suess, R.M. Smith, Morphological Classification of Grass Phytoliths, Soil Sci. Am. Proc. 33 (1969) 109–115. doi:10.1007/s00702-011-0732-4.

[45] P.B. Tomlinson, Anatomy of the monocotyledons. II. Palmae., Clarendon Press Oxford Univ. Press. (1961).

[46] N.N. Brandt, a. Y. Chikishev, K. Itoh, N.L. Rebrikova, ATR-FTIR and FT Raman spectroscopy and laser cleaning of old paper samples with foxings, Laser Phys. 19 (2009) 483–492. doi:10.1134/S1054660X09030220.

[47] P.J. Harris, R.D. Hartley, Detection of bound ferulic acid in cell walls of the Graminae by ultraviolet fluorescence microscopy, Nature 259 (1976) 501–507. doi:10.1038/259508a0.

[48] S. Barsberg, T. Elder, C. Felby, Lignin-quinone interactions: Implications for optical properties of lignin, Chem. Mater. 15 (2003) 649–655. doi:10.1021/cm021162s.

[49] A. Castellan, N. Colombo, A. Nourmamode, J.H. Zhu, D. Lachenal, R.S. Davidson, L. Dunn, Discoloration of α-Carbonyl-Free Lignin Model Compounds Under UV Light Exposure, J. Wood Chem. Technol. 10 (1990) 461–493. doi:10.1080/02773819008050252.

[50] R. Ruggiero, a. E.H. Machado, W. Hoareau, C. Gardrat, A. Nourmamode, S. Grelierb, A. Castellan, Photodegradation of sugarcane bagasse fibers. Influence of acetylation or grafting UVabsorber and/or hindered nitroxide radical on their photostability, J. Braz. Chem. Soc. 17 (2006) 763–770. doi:10.1590/S0103-50532006000400019.

[51] C. Li, X. Zhao, A. Wang, G.W. Huber, T. Zhang, Catalytic Transformation of Lignin for the Production of Chemicals and Fuels, Chem. Rev. 115 (2015) 11559–11624. doi:10.1021/acs.chemrev.5b00155.

[52] J.H. Wiley, R.H. Atalla, Band assignments in the raman spectra of celluloses, Carbohydr. Res. 160 (1987) 113–129. doi:10.1016/0008-6215(87)80306-3.

[53] U.P. Agarwal, Raman imaging to investigate ultrastructure and composition of plant cell walls: Distribution of lignin and cellulose in black spruce wood (Picea mariana), Planta 224 (2006) 1141–1153. doi:10.1007/s00425-006-0295-z.

[54] J. Kolar, M. Strlic, S. Pentzien, W. Kautek, Near-UV, visible and IR pulsed laser light interaction with cellulose, Appl. Phys. A Mater. Sci. Process. 90 (2000) 87–90. doi:10.1007/PL00021097.

Figure captions

Fig. 1 The `angarêb and a detail view of one of its ropes.

Fig. 2 BSE ESEM images of `angarêb samples. TS (a-c) and adaxial surface (d-f).

Fig. 3 Transmitted light and UV-induced Vis fluorescence overall view of lamina (TS) from the `angarêb rope along with a detailed magnification of vascular bundle cells.

Fig. 4 UV induced Vis fluorescence spectra of FL (a-d) and HAL (e-h) samples upon laser irradiation at 532 and 1064 nm (irradiation condition: F_{th}, $2F_{th}$ and $4F_{th}$ at 2 and 10 Hz, respectively). Dotted lines indicate the FL emission of the testing area before irradiation.

Fig. 5 UV induced Vis fluorescence spectra of NAL (a-d) and NALHA (e-h) samples upon laser irradiation at 532 and 1064 nm (irradiation condition: F_{th}, $2F_{th}$ and $4F_{th}$ at 2 and 10 Hz). Dotted lines indicates the FL emission of testing area prior to be irradiated.

Fig. 6 Comparison among pictures taken before and after laser removal of soiling from `angarêb rope samples. Irradiation at 532 and 1064 nm with 11 ns pulses at operative fluences F_{th}, $2F_{th}$, $4F_{th}$ and prr of 2 Hz and 10 Hz. Images sizes are 0.5□0.5 cm^2.

Fig. 7 UV induced Vis fluorescence changes of `angarêb fibers before (dotted) and after (solid) laser irradiation at 532 nm (a-b) and 1064 nm (c-d), and after the subsequent hydrothermal ageing (ef) carried out in order to investigate long-term effects.

Fig. 8 Comparison among Raman spectra of non-irradiated areas (soiled and non-soiled fibers), laser irradiated areas at F_{th}, $2F_{th}$ and $4F_{th}$, and areas hydrothermally aged after irradiation: a) 532 nm, 2Hz; b) 1064 nm, 2Hz; c) 1064 nm, 10Hz; d) 1064 nm, 2Hz then hydrothermal ageing; e) 1064 nm, 10Hz then hydrothermal ageing.


0 15 30
cm

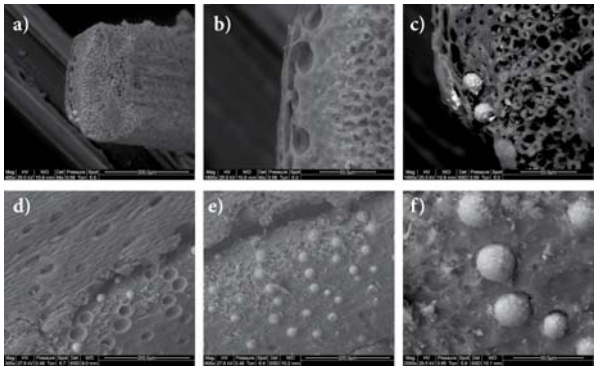
a)
b)
c)
d)
e)
f)

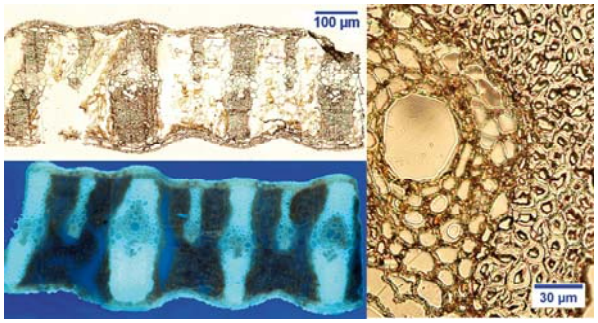
100 µm
30 µm

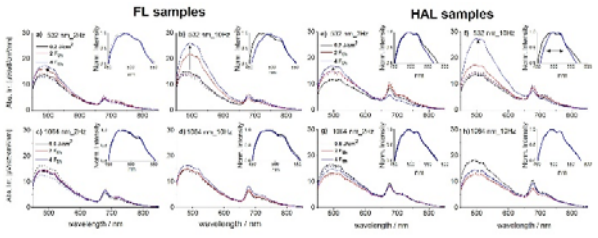
FL samples
HAL samples

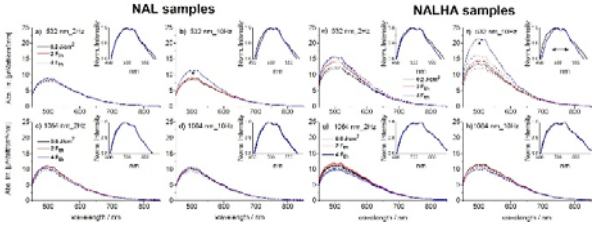
NAL samples
NALHA samples

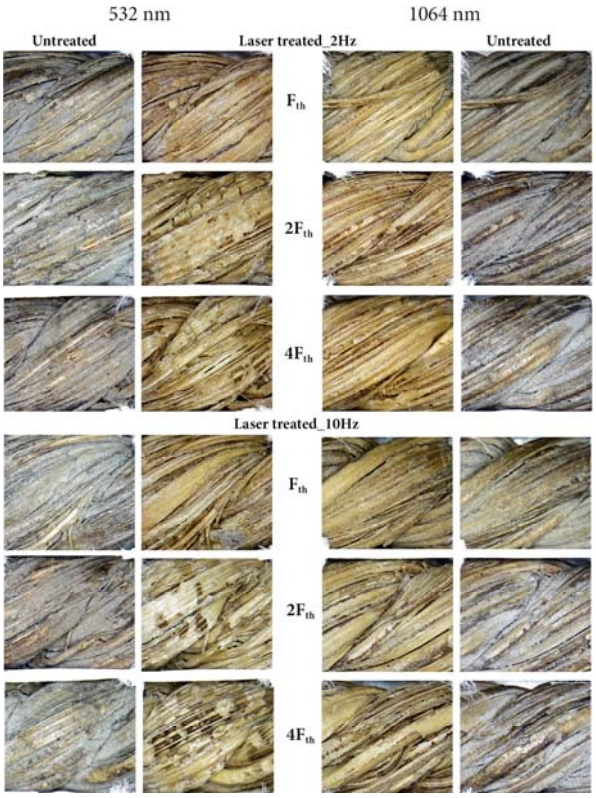
532 nm
1064 nm
Untreated
Laser treated_2Hz
Untreated
Laser treated_10Hz
F_{th}
$2F_{th}$
$4F_{th}$

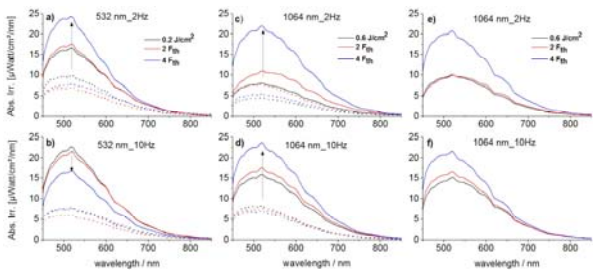
wavelength / nm

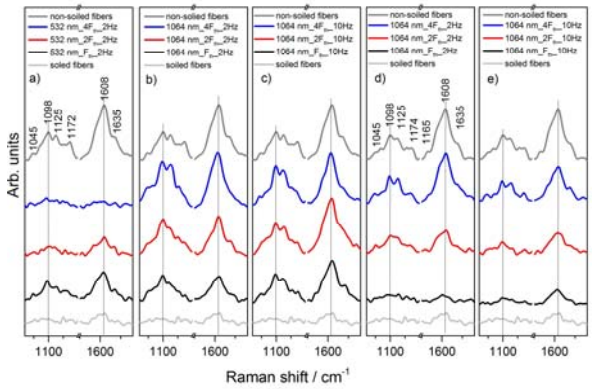
non-soiled fibers
532 nm_4F_pw_2Hz
532 nm_2F_pw_2Hz
532 nm_F_pw_2Hz
soiled fibers
a)
1045
1098
1125
1172
1608
1635
b)
1064 nm_4F_pw_2Hz
1064 nm_2F_pw_2Hz
1064 nm_F_pw_2Hz
c)
1064 nm_4F_pw_10Hz
1064 nm_2F_pw_10Hz
1064 nm_F_pw_10Hz
d)
1174
1165
e)
Arb. units
1100
1600
Raman shift / cm-1

Table 1 Prepared samples of doum palm leaves and fibers. UNI ISO 5630-3 ageing refers to 6 days, at 80 °C and RH 65%.

Sample	Description	Ageing conditions
FL	Fresh leaves	One month in laboratory conditions
HAL	Hydrothermally aged leaves	UNI ISO 5630-3 ageing
NAL	Naturally aged leaves	One year in laboratory conditions
NAF	Naturally aged fibers	One year in laboratory conditions
NALHA	Leaves naturally aged then hydrothermally aged	One year in laboratory conditions then UNI ISO 5630-3 ageing
NAFHA	Fibers naturally aged then hydrothermally aged	One year in laboratory conditions then UNI ISO 5630-3 ageing

Table 1 1608/1098 cm^{-1} band ratio in `angarêb fibers after soiling removal at 1064 nm and subsequent accelerated ageing.

Sample condition	**Non-irradiated**	**Irradiated at 1064 nm_2Hz**			**Irradiated at 1064 nm_10Hz**		
	Non-soiled	F_{th}	$2F_{th}$	$4F_{th}$	F_{th}	$2F_{th}$	$4F_{th}$
Sample as it is	1.14	0.97	1.03	1.10	1.01	1.06	1.15
After ageing	1.13	n.m*	1.20	1.12	n.m	1.10	1.10
n.m*: not measurable							